J|A|C|S COMMUNICATIONS

Published on Web 10/19/2010

Vibrational Predissociation Spectrum of the Carbamate Radical Anion, $C_5H_5N\text{-}CO_2^-$, Generated by Reaction of Pyridine with $(CO_2)_m^-$

Michael Z. Kamrath, Rachael A. Relph, and Mark A. Johnson*

Sterling Chemistry Laboratory, Yale University, P.O. Box 208107, New Haven, Connecticut 06520

Received August 13, 2010; E-mail: mark.johnson@yale.edu

Abstract: We report the vibrational predissociation spectrum of $C_5H_5N\text{-}CO_2^-$, a radical anion which is closely related to the key intermediates postulated to control activation of CO_2 in photoelectrocatalysis with pyridine (Py). The anion is prepared by the reaction of Py vapor with $(CO_2)_m^-$ clusters carried out in an ionized, supersonic entrainment ion source. Comparison with the results of harmonic frequency calculations establishes that this species is a covalently bound molecular anion derived from the corresponding carbamate, $C_5H_5N\text{-}CO_2^-$ (H^+). These results confirm the structural assignment inferred in an earlier analysis of the cluster distributions and photoelectron spectra of the mixed $Py_m(CO_2)_n^-$ complexes [*J. Chem. Phys.* **2000**, *113* (2), 596−601]. The spectra of the $(CO_2)_m^-$ ($m = 5$ and 7) clusters are presented for the first time in the lower energy range (1000−2400 cm^{-1}), which reveal several of the fundamental modes that had only been characterized previously by their overtones and combination bands. Comparison of these new spectra with those displayed by $Py(CO_2)_n^-$ suggests that a small fraction of the $Py(CO_2)_n^-$ ions are trapped entrance channel reaction intermediates in which the charge remains localized on the $(CO_2)_m^-$ part of the cluster.

Very recently, the critical role of N−C bond formation in the activation of CO_2 has been highlighted in the context of the photoelectrochemical conversion of CO_2 to fuels using pyridine (Py) as a catalyst.[1] Although the mechanism is still unclear, a leading hypothesis[2,3] involves the reaction of a transient pyridinium radical, $C_5H_5N-H^{\bullet}$, with CO_2 under reducing conditions to yield the carbamate, $[Py\text{-}CO_2^-(H^+)]$, which effectively occurs by insertion of CO_2 in the N−H bond. This model is supported by experimental work on the $Py_m(CO_2)_n^-$ clusters by Kim and co-workers,[4] who prepared them using electron impact ionization of a supersonic expansion containing Py seeded in CO_2. The unexpected stability of the $PyCO_2^-$ species was evident by the shape of the cluster distribution, and the properties of this 1:1 complex were further explored using photoelectron spectroscopy along with a survey of possible structures obtained using electronic structure calculations. Although the intrinsically broad photoelectron spectrum of $PyCO_2^-$ did not yield any detailed structural features, the value of the vertical electron detachment energy (VDE) of 1.49 eV was close to that of CO_2^- (1.4 eV[5]). This rules out structures based on CO_2 solvation of the Py^- valence ion, which has a VDE of only 0.62 eV. In the course of evaluating structures based on the alternative, CO_2^--based complexes, however, their (UHF) calculations identified an interesting and unexpected covalent form with the structure indicated in Figure 1a, which could account for both the clustering behavior as well as the VDE. In this analysis, the $Py(CO_2)_n^-$ series is based on the covalently bound $PyCO_2^-$ "core ion," with the remaining CO_2 molecules playing the role of a weakly bound solvent. Such a scenario provides an excellent opportunity to carry out a much more refined characterization of the $PyCO_2^-$ anion using vibrational spectroscopy, which becomes available by predissociation of the weakly bound adducts:

$$PyCO_2^-\cdot(CO_2)_q + h\nu \rightarrow PyCO_2^-(CO_2)_p + q-pCO_2 \quad (1)$$

The solvent CO_2 molecules thus act as the mass "messengers" that enable action spectroscopy[6] of the more strongly bound core ion, similar to the situation encountered in our vibrational characterization of the $(C_2O_4^- \leftrightarrow CO_2 + CO_2^-)(CO_2)_m$ cluster system.[7] Here we report vibrational predissociation spectra of $Py(CO_2)_n^-$, $n = 2-4$ and 6, where the ions are prepared in a two-step scheme in which neutral Py is allowed to react with a $(CO_2)_m^-$ cluster beam, thus providing a more controlled synthesis than that used in the earlier work. We then analyze the resulting sharp bands in the context of the harmonic spectra calculated for the structure indicated in Figure 1b.

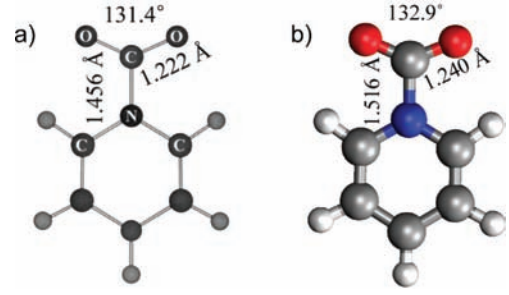

Figure 1. Comparison of the optimized geometries of $PyCO_2^-$ obtained by (a) Kim et al (ref 4) at the UHF/6-311++G(d,p) level of theory and (b) our calculated structure at the B3LYP/6-311++G(d,p) level. Bond lengths and angles are included for key structural parameters.

Vibrational spectra of the $[Py(CO_2)_{n=2-4,6}]^-$ clusters were obtained using Yale's double-focusing, tandem time-of-flight mass spectrometer described previously.[8,9] A pulsed supersonic expansion of neat carbon dioxide (3.8 bar stagnation pressure) was ionized using a 1 keV counter-propagating electron beam, while a mixture of pyridine vapor (298 K) and 1.4 bar argon was entrained[10] into the supersonic flow using a second pulsed valve, whose output is directed into an annular opening located just outside the supersonic orifice. This arrangement has been shown to generate secondary ions arising from collisions between the entrained species and the nascent cluster ions created in the high density region of the main expansion.[10] The resulting ions were then allowed to drift for ∼400 μs before transverse (Wiley−McLaren configuration[11]) acceleration to a final drift energy of ∼2.5 keV. With the entrainment valve turned off, the mass spectrum consists of the well-documented distribution of $(CO_2)_m^-$ cluster ions,[12−16] which is presented in Figure 2a. Introduction of the Ar/Py mixture through the external

10.1021/ja1073036

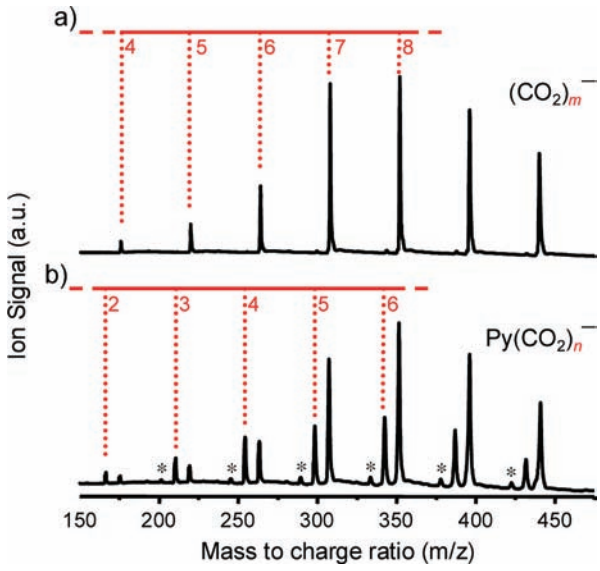

Figure 2. Comparison of typical mass spectra obtained (a) by supersonic expansion of neat CO_2 to form the $(CO_2)_m^-$ cluster series and (b) after introduction of the pyridine/argon mixture into the main CO_2 expansion via entrainment to produce the $Py(CO_2)_n^-$ cluster distribution. The small peaks (*) are of the empirical formula $Py_2(CO_2)_n$ (a.u. = arbitrary units).

pulsed valve yields the extra peaks highlighted in Figure 2b, which correspond to the addition of $m/z = 79$ to $(CO_2)_m^-$ as expected for incorporation of Py. Note that the distribution of these product peaks closely follows that of the precursor $(CO_2)_m^-$ clusters, consistent with their formation by condensation of Py on the homogeneous CO_2 cluster anions upon entrainment. The $PyCO_2^-$ (1:1) complex occurs with about 80% of the ion signal intensity as that of the $Py(CO_2)_2^-$ (1:2) complex.

Vibrational predissociation spectroscopy was carried out using tunable infrared radiation (1000−2400 cm^{-1}) generated with a Nd:YAG pumped OPO/OPA (Laser Vision). This source utilizes parametric conversion in $AgGaSe_2$ and delivers 50 to 500 μJ/pulse over the course of the scan, with the lowest output power occurring at the low frequency limit. The reported spectra result from accumulation of 5−10 individual scans and are displayed as the net fragment ion yield, normalized to the laser energy/pulse across the scanned frequency range. The uncertainty in the reported band positions is ~5 cm^{-1} due to the laser bandwidth (2 cm^{-1}) and scan reproducibility.

Geometry optimization and (harmonic) vibrational frequency calculations were performed using Gaussian 03.[17] Density functional theory was carried out at the B3LYP/6-311++G(d,p) level for both the $PyCO_2^-$ and $Py(CO_2)_2^-$ anions to obtain vibrational information on these systems. The frequencies reported here have not been scaled.

Since the synthesis of the $Py(CO_2)_n^-$ products involves reaction of neutral Py with $(CO_2)_m^-$,

$$Py + (CO_2)_m^- \rightarrow Py(CO_2)_n^- + (m-n)CO_2 \qquad (2)$$

it is useful to consider the spectral properties of all species involved in order to identify the region of the vibrational spectrum that provides the most definitive signature of covalent bond formation in $PyCO_2^-$. This involves minimizing complications arising from overlap of the bands expected for the carbamate with transitions in the reactants or spectator CO_2 solvent in the product.

Identifying the optimal spectral region for product analysis requires careful consideration of the special complexities associated with the $(CO_2)_m^-$ reactant anions. Electron attachment to homogeneous neutral CO_2 clusters yields the anionic analogues in which the excess charge is localized on either the monomer (CO_2^-) or dimer ($C_2O_4^-$) molecular cores in a highly size-dependent manner.[7,13,18−20] Earlier work relying on $(CO_2)_m^-$ photoelectron spectroscopy[13] and the patterns of overtones and combinations in the high frequency (2300−3800 cm^{-1}) vibrational predissociation spectrum[7] has identified $m = 5$ and 7 as examples of species with relatively pure dimer and monomer core ions, respectively. We therefore recorded the spectra of these archetypal clusters in the region of their IR fundamentals, with the results displayed in Figure 3a and 3b for $m = 7$ and 5, respectively, and the positions of the most prominent features collected in Table 1. These spectra were recorded by monitoring the loss of a single CO_2 molecule.

Both the $m = 5$ and 7 clusters are formed with several CO_2 molecules playing the role of a solvent around the core ion, and this is immediately evident in their spectra (Figure 3) by the strong band associated with the antisymmetric C−O stretch at 2349 cm^{-1} (arrows in top trace indicate the ν_1 and ν_3 locations in the isolated CO_2 molecule). Note that there is little absorption in the vicinity of the CO_2 symmetric stretch (ν_1), establishing that this forbidden transition is not significantly enhanced by symmetry breaking in the clusters. The spectrum of the monomer core cluster ($m = 7$, Figure 3a) features a very strong band at 1660 cm^{-1} that has been assigned to the asymmetric stretching mode of the bent O−C−O core molecular anion. Note that this appears far below the corresponding ν_3 mode in neutral CO_2, as the excess electron acts to weaken the bonding in the radical anion. This absorption blue shifts by about 200 cm^{-1} upon formation of the $C_2O_4^-$ dimer core in the $m = 5$ system (Figure 3b), qualitatively reflecting the delocalization of antibonding character among the two CO_2 constituents.[21,22]

Having established the spectral signatures of the $(CO_2)_m^-$ reactant ions, we turn our attention to the predicted vibrational spectrum of the covalently bound $PyCO_2^-$ radical ion indicated in Figure 1b. The calculated harmonic spectrum of this species is indicated in Figure 3d, while the fundamentals in the fingerprint region are included in Table 1. It indeed exhibits a very strong band at 1270 cm^{-1} that appears in a quiet window in the spectra of both the monomer and dimer-based $(CO_2)_m^-$ reactant clusters as well as that

Table 1. Experimental Frequencies for the Carbamate Anion Series $Py(CO_2)_n^-$, $n = 2-4$, 6, and Neat $(CO_2)_5^-$ and $(CO_2)_7^-$ Clusters[a]

		Frequencies, cm^{-1}					
Method	Species	Py ring deformation	C−N stretch	CO_2^- ν_3	−N-CO_2^- ν_3	$C_2O_4^-$	free CO_2 ν_3
Experimental	Py-CO_2^-·(CO_2)		1266		1715		2331
	Py-CO_2^-·$(CO_2)_2$	1093	1271		1705	1861, 1884	2337
	Py-CO_2^-·$(CO_2)_3$	1097	1279		1699		2338
	Py-CO_2^-·$(CO_2)_5$	1108	1289	1650	1685		2341
	$(CO_2)_5^-$	N/A	N/A		N/A	1865, 1904	2349
	$(CO_2)_7^-$	N/A	N/A	1660	N/A		2349
Calculated	$Py(CO_2)^-$	1081	1270		1765		N/A
	$Py(CO_2)_2^-$	1098	1283		1739		2398

[a] Calculated (B3LYP/6-311++G(d,p)) fundamentals are also included for $Py(CO_2)_n^-$, $n = 1$ and 2.

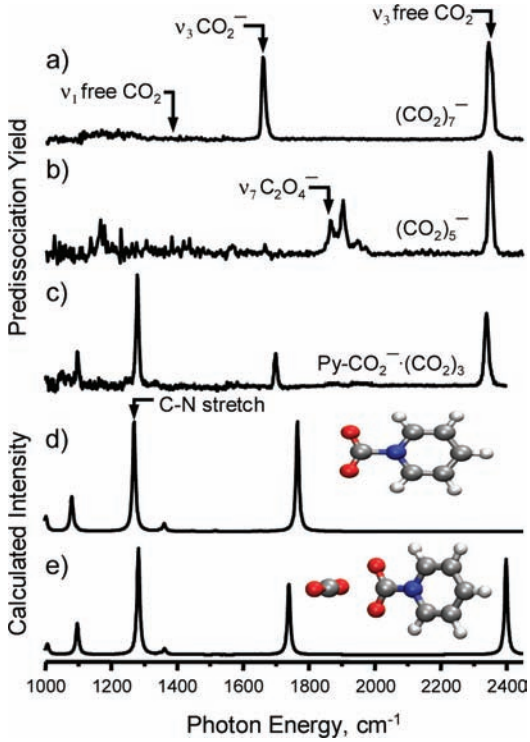

Figure 3. Vibrational predissociation spectra of $(CO_2)_m^-$ reactant species (a) $(CO_2)_7^-$ and (b) $(CO_2)_5^-$ which have monomer and dimer cores, respectively, as well as the predissociation spectrum of (c) Py-CO_2^-·$(CO_2)_3$ for comparison. Calculated geometries and harmonic spectra (B3LYP/6-311++G(d,p)) are also shown for (d) Py$(CO_2)^-$ and (e) Py$(CO_2)_2^-$.

of neutral Py.[23] Moreover, the displacements involved in this transition are primarily due to the critical C−N stretching motion and, thus, directly reflect the character of the covalent bond.

Photoexcitation of the PyCO_2^- (1:1) complex did not display any photofragmentation throughout the fingerprint region, consistent with its identification as a distinct, strongly bound "core ion." The larger clusters, Py$(CO_2)_n^-$, $n = 2-4$, 6, on the other hand, could be photodissociated in this region through the loss of a single CO_2 molecule, consistent with the photoevaporation behavior of the $(CO_2)_m^-$ clusters described above.[7,15,24,25] Figure 3c presents the resulting vibrational predissociation spectrum of the Py$(CO_2)_4^-$ cluster. In addition to the expected 2338 cm^{-1} band due to ν_3 of the neutral CO_2 solvent molecules, there are three strong transitions with locations and relative intensities quite close to those calculated for the covalently bound PyCO_2^- anion. In particular, a very intense band is recovered in the position expected for the key C−N stretching vibration at 1279 cm^{-1}. The fact that that this new band is not present in either of the reactants thus confirms the suggestion in the previous work[4] that the product clusters occur predominantly as Py-CO_2^-·$(CO_2)_{n-1}$, with the Py-CO_2^- core ion occurring with the structure indicated in Figure 1.

The close proximity of the solvent CO_2 transition to its position in the isolated molecule indicates that these spectator molecules are not strongly perturbed by the presence of the ion. Based on the photofragmentation behavior,[15,24] the bond energy is rather large (on the order of 1700 cm^{-1}), and it is important to gauge the extent to which the anion is perturbed by the proximity of the CO_2 solvent molecules. We address this issue using theoretical analysis complemented by an experimental study of the size dependence of the bands in the series: Py$(CO_2)_n^-$, $n = 2-4$ and 6.

To identify the likely location of the CO_2 binding site and to gauge the degree of PyCO_2^- perturbation caused by complexation, we carried out electronic structure calculations (B3LYP/6-311++G(d,p)) on the Py-CO_2^-·CO_2 (1:2) system and recovered the minimum energy structure and harmonic spectrum displayed in Figure 3e. Note that this configuration features attachment at the $-CO_2^-$ functionality, with the CO_2 neutral axis oriented 90° relative to the plane of the radical anion. The harmonic spectrum recovers the observed strong band arising from the ν_3 band of the solvent, while the transitions intrinsic to the Py-CO_2^- ion display only minor shifts (∼13 cm^{-1}) and intensity variations. The C−N band at 1283 cm^{-1} is particularly insensitive to solvation, while the higher energy band (1765 cm^{-1}) arising from the O−C−O asymmetric stretch is the most red shifted (26 cm^{-1}), which interestingly brings it even closer to the experimental transition at 1705 cm^{-1}. The calculated pattern also includes the ν_1 mode of the spectator CO_2 molecule, which is indeed quite weak (as it was in the $(CO_2)_m^-$ clusters) and is predicted to appear about 82 cm^{-1} to the blue of the strong C−N stretching band. From the theoretical perspective, then, we do not expect CO_2 solvation to qualitatively change our initial conclusion that the C−N covalent bond has formed in PyCO_2^-. That is, the key spectral signature associated with the C−N linkage is expected to be robust with respect to solvent shifts.

The empirical solvation behavior was also explored by following the size dependence of the Py-CO_2^-·$(CO_2)_{n-1}$ predissociation spectra, with the results displayed in Figure 4. Most importantly, the three strong bands assigned to the Py-CO_2^- anion are present in all cases. The O−C−O asymmetric stretch near 1700 cm^{-1} displays the largest incremental red shift (∼7 cm^{-1}/CO_2) while the C−N stretch blue shifts at a similar rate (∼6 cm^{-1}/CO_2).

Finally, we note that the ∼1700 cm^{-1} band, nominally the O−C−O asymmetric stretching transition of Py-CO_2^-, is quite close to a feature in the spectrum of the $(CO_2)_7^-$ cluster which occurs with the CO_2^- monomer core (Figure 3a; see also Table 1). The proximity of these bands is not surprising, since the transitions both involve the same type of motion in the $-CO_2^-$ motif. In light of this situation, however, it is interesting that, upon inspection of the Py-CO_2^-·$(CO_2)_5$ spectrum in Figure 4d, the $-CO_2^-$ band appears as a close doublet with the low energy feature (arrow in (d)) falling at almost the same location as the band in the $(CO_2)_7^-$ spectrum shown in Figure 3a. It is possible that the extra band arises from solvent perturbation involving different arrangements of the CO_2 solvent at this size, but it is curious that the doubling only occurs in the Py-CO_2^-·$(CO_2)_5$ spectrum. This strong size dependence raises another interesting possibility, however, that the Py$(CO_2)_n^-$ ion ensemble created by reaction 2 is heterogeneous such that it retains an unreacted component in which neutral Py solvates the $(CO_2)_m^-$ moiety with a monomer core. This would naturally explain the size dependence because it is known that the $(CO_2)_m^-$ clusters display a "core switching" behavior from monomer to dimer with decreasing cluster size in the neighborhood of $m = 5$.[7,13,18] With that in mind, we note that the doublet disappears in the spectrum of the smaller Py$(CO_2)_3^-$ cluster (Figure 4b), while a new band (arrow in (b)) emerges at the same location as the spectral signature of the $C_2O_4^-$ dimer anion (Figure 3b). We therefore suggest that a small fraction of the collisions in reaction 2 occur such that the core ion in the $(CO_2)_m^-$ reactant remains intact, and the Py$(CO_2)_n^-$ species created by this path represent captured reaction intermediates in the charge-transfer process leading to C−N bond formation. This, in turn, suggests that there is a barrier in the potential energy landscape governing C−N bond formation in the cluster regime. If this hypothesis is correct, this unreactive fraction should not display the C−N stretching band, a prediction that can be checked by double-resonance methods.[26] This more challenging

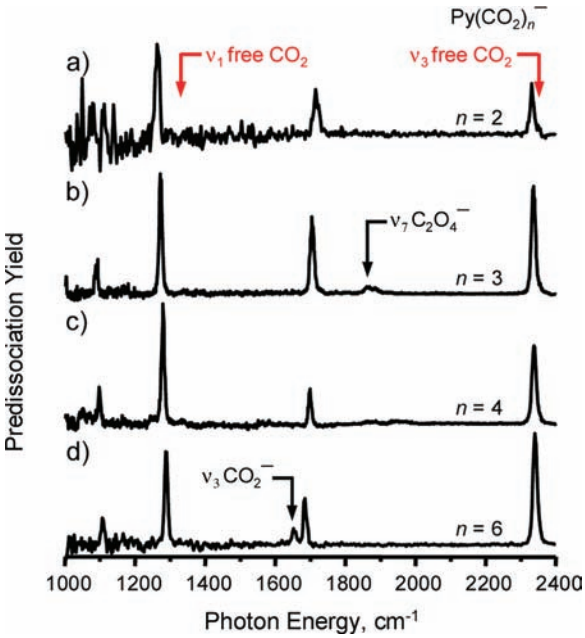

Figure 4. Vibrational predissociation spectra of $Py(CO_2)_n^-$, $n = 2-4$ and 6, obtained by monitoring the loss of a CO_2 molecule. Arrows indicate the positions of the symmetric and antisymmetric stretching bands of neutral CO_2 at 1333 and 2349 cm^{-1}, respectively, in (a), while arrows in (b) and (d) denote the signatures of the $C_2O_4^-$ and CO_2^- core ions, respectively.

experiment will be a useful next step in the characterization of the reaction dynamics at the heart of C−N bond formation.

Acknowledgment. We thank the Air Force Office of Scientific Research under Grant FA-9550-09-1-0139 and the Department of Energy under Grant DE-FG02-06ER15800 for their support of this work, which effectively leverages our long-standing efforts in excess electron accommodation to provide a new window on the mechanisms of CO_2 activation.

Supporting Information Available: Complete ref 17. This material is available free of charge via the Internet at http://pubs.acs.org.

References

(1) Barton, E. E.; Rampulla, D. M.; Bocarsly, A. B. *J. Am. Chem. Soc.* **2008**, *130*, 6342–6344.
(2) Cole, E. B. Ph.D. Thesis, Princeton University, Princeton, 2009; p 135.
(3) Cole, E. B.; Lakkaraju, P. S.; Rampulla, D. M.; Morris, A. J.; Abelev, E.; Bocarsly, A. B. *J. Am. Chem. Soc.* **2010**, *132*, 11539–11551.
(4) Han, S. Y.; Chu, I.; Kim, J. H.; Song, J. K.; Kim, S. K. *J. Chem. Phys.* **2000**, *113*, 596–601.
(5) Arnold, S. T.; Coe, J. V.; Eaton, J. G.; Freidhoff, C. B.; Kidder, L.; Lee, G. H.; Manaa, M. R.; Mchugh, K. M.; Patel-Misra, D.; Sarkas, H. W.; Snodgrass, J. T.; Bowen, K. H. In *The Chemical Physics of Atomic and Molecular Clusters*; Scoles, G., Ed.; North-Holland: Amsterdam, 1990.
(6) Okumura, M.; Yeh, L. I.; Myers, J. D.; Lee, Y. T. *J. Chem. Phys.* **1986**, *85*, 2328–2329.
(7) Shin, J.-W.; Hammer, N. I.; Johnson, M. A.; Schneider, H.; Gloss, A.; Weber, J. M. *J. Phys. Chem. A* **2005**, *109*, 3146–3152.
(8) Posey, L. A.; Johnson, M. A. *J. Chem. Phys.* **1988**, *89*, 4807–4814.
(9) Johnson, M. A.; Lineberger, W. C. In *Techniques for the Study of Ion−Molecule Reactions*; Farrar, J. M., Saunders, W. H., Jr., Eds.; Wiley: New York, 1988; Vol. XX, p 591.
(10) Robertson, W. H.; Kelley, J. A.; Johnson, M. A. *Rev. Sci. Instrum.* **2000**, *71*, 4431–4434.
(11) Wiley, W. C.; McLaren, I. H. *Rev. Sci. Instrum.* **1955**, *26*, 1150–1157.
(12) Sudoh, K.; Matsuyama, Y.; Muraoka, A.; Nakanishi, R.; Nagata, T. *Chem. Phys. Lett.* **2006**, *433*, 10–14.
(13) DeLuca, M. J.; Niu, B.; Johnson, M. A. *J. Chem. Phys.* **1988**, *88*, 5857–5863.
(14) Tsukuda, T.; Saeki, M.; Iwata, S.; Nagata, T. *J. Phys. Chem. A* **1997**, *101*, 5103–5110.
(15) Alexander, M. L.; Johnson, M. A.; Levinger, N. E.; Lineberger, W. C. *Phys. Rev. Lett.* **1986**, *57*, 976.
(16) Johnson, M. A.; Alexander, M. L.; Lineberger, W. C. *Chem. Phys. Lett.* **1984**, *112*, 285–290.
(17) Frisch, M. J. *Gaussian 03*; Gaussian, Inc.: Wallingford, CT, 2004.
(18) Tsukuda, T.; Johnson, M. A.; Nagata, T. *Chem. Phys. Lett.* **1997**, *268*, 429–433.
(19) Muraoka, A.; Inokuchi, Y.; Hammer, N. I.; Shin, J. W.; Johnson, M. A.; Nagata, T. *J. Phys. Chem. A* **2009**, *113*, 8942–8948.
(20) Fleischman, S. H.; Jordan, K. D. *J. Phys. Chem.* **1987**, *91*, 1300.
(21) Zhou, M.; Andrews, L. *J. Chem. Phys.* **1999**, *110*, 2414.
(22) Thompson, W. E.; Jacox, M. E. *J. Chem. Phys.* **1999**, *111*, 4487.
(23) Wong, K. N.; Colson, S. D. *J. Mol. Spectrosc.* **1984**, *104*, 129–151.
(24) Alexander, M. L.; Johnson, M. A.; Lineberger, W. C. *J. Chem. Phys.* **1985**, *82*, 5288–5289.
(25) Engelking, P. C. *J. Chem. Phys.* **1987**, *87*, 936.
(26) Elliott, B. M.; Relph, R. A.; Roscioli, J. R.; Bopp, J. C.; Gardenier, G. H.; Guasco, T. L.; Johnson, M. A. *J. Chem. Phys.* **2008**, *129*, 094303.

JA1073036